

# Dark matter halo concentrations with a bayesian approach

Christian Poveda<sup>1</sup> & Jaime E. Forero-Romero<sup>1</sup>

<sup>1</sup>*Departamento de Física, Universidad de los Andes, Cra. 1 No. 18A-10, Edificio Ip, Bogotá, Colombia*

24 August 2014

## ABSTRACT

asd

**Key words:** methods: numerical, galaxies: haloes, cosmology: theory, dark matter

## 1 INTRODUCTION

(Navarro et al. 1997)

## 2 BASIC PROPERTIES OF THE NFW DENSITY PROFILE

The Navarro-Frenk-White density profile can be written as

$$\rho(r) = \frac{\rho_c \delta_c}{r/r_s (1 + r/r_s)^2}, \quad (1)$$

where  $\rho_c \equiv 3H^2/8\pi G$  is the Universe critical density,  $\delta_c$  is the halo dimensionless characteristic density and  $r_s$  is known as the scale radius, the radius that marks the transition between the two power law behaviour in the  $\rho \propto r^{-1}$  for  $r < r_s$  and  $\rho \propto r^{-2}$  for  $r > r_s$ .

We define the virial radius of a halo,  $r_v$ , as the boundary of the spherical volume that encloses an average density of  $\Delta_h$  times the average density of the Universe. The corresponding mass  $M_v$ , the virial mass, can be thus expressed as  $M_v = \frac{4\pi}{3} \bar{\rho} \Delta_h r_v^3$ .

The total mass enclosed within a radius  $r$  can be computed to be:

$$M(< r) = 4\pi \rho_c \delta_c r_s^3 \left[ \ln \left( \frac{r_s + r}{r} \right) - \frac{r}{r_s + r} \right]. \quad (2)$$

We can now define the concentration of the halo as  $c = r_v/r_s$ , the dimensionless variable  $x \equiv r/r_v$  and  $m \equiv M(< r)/M_v$ , which allows us to express the total enclosed mass within a dimensionless radius  $x$  as:

$$m(< x) = \frac{1}{A} \left[ \ln(1 + xc) - \left( \frac{xc}{xc + 1} \right) \right], \quad (3)$$

where

$$A = \left[ \ln(1 + c) - \left( \frac{c}{c + 1} \right) \right], \quad (4)$$

meaning that the concentration is the only free parameter to determine the density profile of the halo. In Figure 1

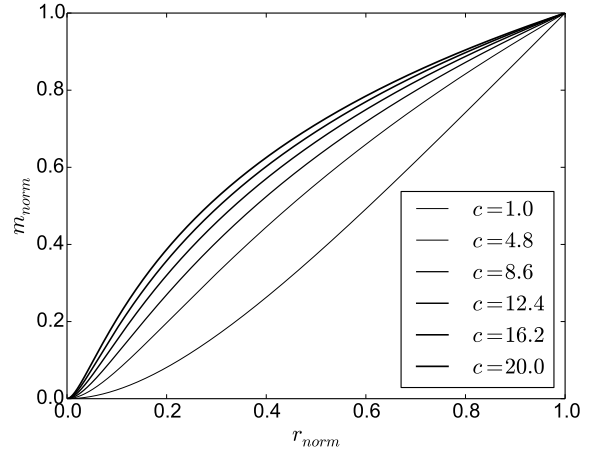


**Figure 1.** Mass profiles of several haloes with different concentrations

we show the family of normalized integrated mass profiles for different values of the concentration in the range  $1 \leq c \leq 20$ .

## 3 A BAYESIAN APPROACH TO HALO FITTING

We proceed to find the value of the concentration parameter that best describes the simulation data, following the model in Eq. (3). We use the integrated mass profile because it allows us to use the data directly with the simulation without binning the particle positions and estimating a density.

We construct the integrated mass profile by ranking the particles by their increasing distance to the center of the halo. Once they are ranked, the total mass at a radius  $r_i$ , increases by  $m_p$ , where  $r_i$  is the position of the  $i$ -th particle and  $m_p$  is the mass of the computational particle. We define the center of the halo to be at the position of the particle with the lowest gravitational potential. In the process

of building the mass profile we discard the particle at the center.

We stop the construction of the integrated mass profile once we arrive at an average density of  $\Delta_h \bar{\rho}$ . This radius marks the virial radius and the virial mass. We divide the total mass enclosed mass  $M_i$  and the radii  $r_i$  by these values to obtain the dimensionless variables  $x_i$  and  $m_i$ .

Using these positions and masses we define the following  $\chi^2$  function

$$\chi^2(c) = \sum_i [\log m_i - \log m(< x_i; c)]^2, \quad (5)$$

where  $m(< x_i; c)$  corresponds to the values in Eq.(3) at  $x = x_i$  and a given value of the concentration parameter  $c$ .

Finally we use a Metropolis-Hastings algorithm to sample the likelihood function distribution defined by  $\mathcal{L}(c) = \exp(-\chi^2(c)/2)$  to find the optimum value of  $c$  and its associated uncertainty  $\sigma_c$ .

## 4 NUMERICAL EXPERIMENTS

### 4.1 Mock Halos

We generate 100 mock halos with concentration values randomly placed in the range  $1 < c < 10$ . Each one of the halos is generated with four different total particle numbers: 20, 200, 2000 and 20000.

The method we use to generate the halos is based on the integrated mass profile. Given the number of particles  $n$  and the concentration  $c$  we define the mass element as  $\delta m = 1/n$  (this corresponds to the mass of each particle such that the total mass is one). Then for each number  $k$  from 1 to  $n$  we find the value of  $r$  such that the difference

$$m(< r; c) - k \cdot \delta m \quad (6)$$

is zero using Ridders' method. This value of  $r$  is the radius of the  $k$ th particle of the generated halo, then polar and azimuthal angles  $\theta$  and  $\phi$  are randomly generated. Finally these three coordinates are transformed into cartesian coordinates  $(r, \theta, \phi) \rightarrow (x, y, z)$ . This process is repeated  $n$  times in order to generate the  $x, y, z$  coordinates for each particle.

### 4.2 Simulation Data

We use data from the MultiDark cosmological volume. This simulation follows the non-linear evolution of a dark matter density field sampled with  $2048^3$  particles over a cubic box of  $1000 h^{-1} \text{Mpc}$  on a side. The data is publicly available, more details about the structure of the database and the simulations can be found in (Riebe et al. 2013).

We select a sample of halos in a cubic sub-volume of  $100 h^{-1} \text{Mpc}$  on a side centered on the most massive halo in the simulation at  $z = 0^1$ . We select first all the halos at  $z = 0$  detected with a Friends-of-Friends (FoF) algorithm with masses in the interval  $10^{11} \leq M_{\text{FoF}}/h^{-1} \text{M}_\odot \leq 10^{15}$ . The FoF algorithm ran with a linking length of 0.17 times the average interparticle distance. This choice translates into

<sup>1</sup> This corresponds to the *miniMDR1* database in the MultiDark webpage

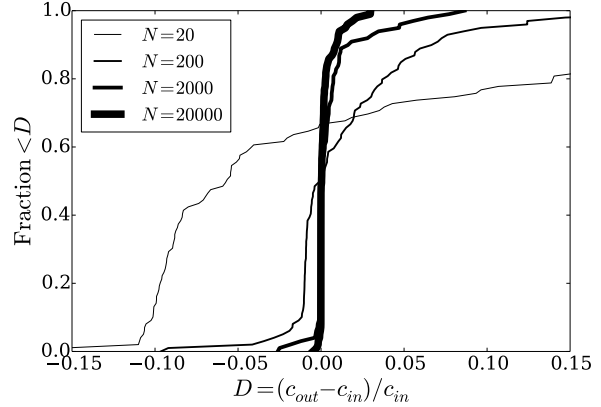


**Figure 2.** Cumulative distribution of the fractional difference between the input concentration in the mock halo generator,  $c_{in}$  and the measurement by our MCMC code,  $c_{out}$ . Each curve corresponds to halos generated with a different number of particles,  $N$ .

an overdensity  $\Delta_h \sim 400 - 700$  that is dependent on the halo concentration (More et al. 2011).

For each selected halo with the previous procedure we select from the database all the particles that belong to it. From the particles we follow the procedure spelled out in Section 3 with  $\Delta_h = 740$  (corresponding to 200 times the critical density) to find the halo concentration. Finally, we store the values obtained for the virial radius, virial mass and concentration.

## 5 RESULTS

### 5.1 Mock Halos

In Figure 2 we show the integrated distribution percentual difference between the concentration measured with our fitting method  $c_{out}$  in comparison with the concentration used to generate the mock halos,  $c_{in}$ ,  $D = (c_{in} - c_{out})/c_{in}$ . Then we can see that as the number of particles increases, the curve becomes more pronounced at 0. Showing that for most of the halos  $c_{in}$  is very similar to  $c_{out}$ .

### 5.2 Simulation Data

## 6 DISCUSSION

### 6.1 Comparison against other methods

We compared this method against two methods: The first one consists in using shells for estimating the density in function of the radius and using the same MCMC method for fitting and the second one consists in using the circular velocity  $V(r) = \sqrt{GM(< r)/r}$  and the relation for the NFW profile

$$\frac{V_{max}}{V(r_{vir})} = \sqrt{\frac{0.216c}{M(r_{vir})}} \quad (7)$$

Where  $V_{max}$  is the maximum velocity, to find the value of the concentration. We obtained the following results

Fixme: RESULTS!

## 6.2 Concentration as a function of halo mass

Additionally we compared those three methods plotting the concentration as a function of halo mass

Fixme: Plot!

The bold lines in Figure ?? corresponds to the median and the thinner lines corresponds to the quartiles.

## 6.3 Implication for comparisons against observations

FIXME: Ask to Jaime

## 7 CONCLUSIONS

FIXME: Ask to Jaime

## REFERENCES

- More S., Kravtsov A. V., Dalal N., Gottlöber S., 2011, ApJS, 195, 4  
Navarro J. F., Frenk C. S., White S. D. M., 1997, ApJ, 490, 493  
Riebe K., Partl A. M., Enke H., Forero-Romero J., Gottlöber S., Klypin A., Lemson G., Prada F., Primack J. R., Steinmetz M., Turchaninov V., 2013, Astronomische Nachrichten, 334, 691